**Mostefa KOULALI[1], Karim NEGADI[2], Mohamed MANKOUR[1], Abdelkader MEZOUAR[1],
Abderrahmane BERKANI[2], Bachir BOUMEDIENE[2]**

Electrotechnical Engineering Laboratory, University Tahar Moulay of Saida (1), Laboratory of L2GEGI, University Ibn Khaldoun of Tiaret (2)

Adaptive Fuzzy Control of Hybrid PV/Fuel Cell and Battery System using Three-Level T type Inverter

Abstract. This work deals with the study of an electrical energy production system made up of three sources of energy: photovoltaic energy, a fuel cell and a battery. The optimization of this hybrid production system is ensured by the control of each part. The hybrid system chain also contains a three level T type inverter that improves the quality of energy injected into the alternating load and consequently reduces the harmonic rate. The Renewable Energy Management System provides a global overview of the performance of the hybrid system and allows for a quick analysis to understand the root causes of a problem, an improvement in efficiency through a comparison of power curves as well as a visualization of trends in production. The considered system was implemented in the Matlab / Simulink, the results show the effectiveness of the proposed method. In order to optimize the power flow in the different parts of the production line, an energy management algorithm is developed in order to mitigate the fluctuations of the load. To analyze our approach, a prototype is modelled, simulated with Matlab / simulink and can be realized in an experimental test bench

*Streszczenie. Praca dotyczy badania systemu produkcji energii elektrycznej złożonego z trzech źródeł energii: energii fotowoltaicznej, ogniwa paliwowego i baterii. Optymalizację tego hybrydowego systemu produkcji zapewnia kontrola każdej części. Łańcuch systemu hybrydowego zawiera falownik T trzeciego poziomu, który poprawia jakość energii w przemiennym obciążeniu i zmniejsza częstotliwość harmonicznych. System zarządzania energią odnawialną zapewnia kompleksowy obraz wydajności systemu hybrydowego i pozwala na szybką analizę przyczyn problemu, poprawę wydajności poprzez porównanie mocy i wizualizacji trendów produkcyjnych. . Rozważany system został zaimplementowany w Matlab / Simulink, wyniki pokazują skuteczność proponowanej metody. Aby zoptymalizować przepływ mocy linii produkcyjnej, opracowano algorytm zarządzania energią w celu zmniejszenia wahań obciążenia. Aby przeanalizować nasze podejście, modeluje się prototyp, symuluje za pomocą Matlab / simulink i można go zrealizować w eksperymentalnej ławce testowej. **Adaptacyjny algorytm sterowania hybrydowym systemem wytwarzania energii wykorzystujący falownik typu T i logikę rozmytą***

Keywords: Fuell Cell, Photovoltaic PV, Battery, Hybrid System, Three Level T type Inverter, Adaptive Fuzzy Logic Control (AFLC).
Słowa kluczowe: Ogniwo, fotowoltaiczne PV, akumulator, układ hybrydowy, trójpoziomowy falownik typu T, adaptacyjne sterowanie rozmyte (AFLC).

Introduction

The Renewable Energy Management System includes a set of integrated tools to maximize power generation, increase availability, control energy loss and improve overall operational performance. The major objectives of these approaches are to have reduced environmental damage, conservation of energy, exhaustible sources and increased safety. The renewable energy systems can be used to supply power either directly to a utility grid or to an isolated load [1].

The integration of Energy storage systems (ESSs) have some significant applications in operations like grid stabilization, stable power quality, load shifting, grid operational support and smooth power injection to grid. Several power smoothing methods have been introduced in literature [2], battery energy storage system (BESS) is selected as energy storage and incorporated into fuel cell, PV to maintain power and energy balance as well as to improve power quality.

In our research, the proposed Energy Management of multi-sources Power System PV/Fuel Cell and Battery Based Three Level T type Inverter consists of a fuel cell energy conversion system FC/PV generators as the primary energy source and a battery energy storage system (as short and medium, time storage devices).

They are all connected to a DC voltage link, and a three phase three level T type inverter is used to connect the whole system to the load. The DC coupled structure makes the overall system more flexible since the number and the types of energy sources can be freely chosen and it requires fewer controllers as no synchronization is needed to integrate the energy sources.

Regarding the control of the three-level T type inverter connected to the load, we used fuzzy logic control (FLC) to ensure the RMS value of the load voltage.

The structure of the presented work is organized as follow: The description of the study system and the physical modelling of different part with their equations model is set in section 2. The control of different component is set in section 3. The simulations results of the studied are presented in section 4. Section 5 summarizes the work done in the conclusion.

Description of the studied system

The studied system contains the elements that appear in figure 1, the modelling of each element of the chain of conversion will be presented below.
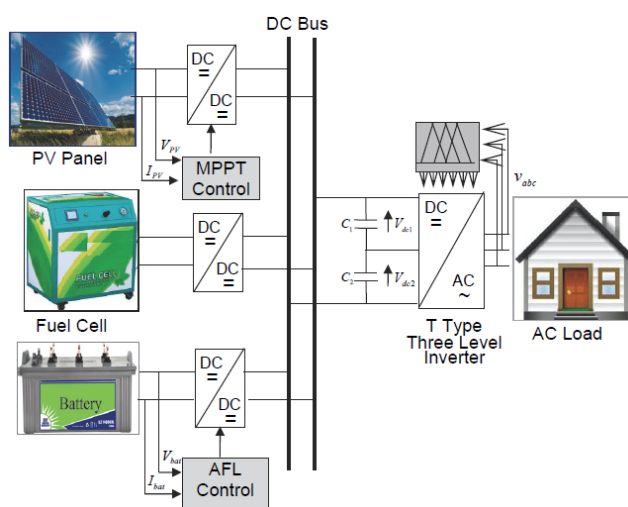

Fig. 1. Synoptic diagram of the studied system

Modelling and Control of System Components

The multi-sources system shown in figure 1 contains control strategies that will be developed in this section.

Modelling of Fuel Cell

A dynamic model of the PEMFC is based on the relationship between the output voltage and potential pressure of hydrogen, oxygen and water. The overall output voltage of the fuel cell stack can be obtained as [13, 14].

(1) $$V_{cell} = E_{nerst} - V_{act} - V_{ohmic} - V_{con}$$

Where E_{nerst} is the Nernst voltage, which is the thermodynamics voltage of the cells and depends on the temperatures and partial pressures of reactants and products inside the stack, E_0 is the standard reversible cell potential (V), N_0 is number of cells in stack, R is the universal gas constant (8.3145 J·mol^{-1}·K^{-1}), T is the stack temperature (K) , F is the Faraday's constant (96485 A·C·mol^{-1}), $P_{H_2}, P_{O_2}, P_{H_2O}$, are the partial pressures of hydrogen, oxygen and water (atm) respectively.

(2)
$$\begin{cases} E_{nerst} = N_0[E_0 + \dfrac{RT}{2F}\log(\dfrac{P_{H2}\, p_{O2}^{0.5}}{P_{H2O}})] \\ V_{ohmic} = R_m I \end{cases}$$

Where $K_{O_2}, K_{H_2}, K_{H_2O}$ are the valve molar constant for oxygen, hydrogen and water in (Kmol·s^{-1}·atm^{-1}) respectively.

(3)
$$\begin{cases} P_{O2} = \dfrac{1/k_{O2}}{1+\tau_{O2}s}(q_{O2}^{in} - 2k_r I) \\ p_{H2} = \dfrac{1/K_{H2}}{1+\tau_{H2}s}(q_{H2}^{in} - 2k_r I) \\ P_{H2O} = \dfrac{1/K_{H2O}}{1+\tau_{H2O}s}(2K_r I_{fc}) \\ q_{H2}^{in} = \dfrac{1}{1+T_f s}[\dfrac{2k_r}{U_{opt}} I_{fc}) \\ q_{O2}^{in} = \dfrac{1}{rHO} q_{H2}^{in} \end{cases}$$

$q_{H_2}^{in}, q_{O_2}^{in}$ and are the hydrogen and oxygen input flow (kMol/s), I is the stack current (A), $K_r = \dfrac{N}{4F}$ is the modeling constant, with N being the number of the series –wound fuel cells in the stack. $\tau_{H_2}, \tau_{O_2}, \tau_{H_2O}$ are the time constants for hydrogen , oxygen and water in (sec), U_{opt} is the optimum fuel utilization , T_f is the fuel time constant (sec), rHO is ratio of hydrogen to oxygen [13,14], $V_{act}, V_{ohmic}, V_{con}$ are the activation, Ohmic and concentration polarizations losses respectively.

(4) $V_{act} = [\xi_1 + \xi_2 T + \xi_{3T} \times \ln(C_{O2}) + \xi_4 T \times \ln(I)]$

Where $\xi_i\left(i=1,2,3,4\right)$ are the parametric coefficients defined based on the kinetic, thermodynamic and electrochemical phenomena. Co_2 is the concentration of oxygen dissolved in a water film interface in the catalytic of the cathode in (mol/m^3). It is expressed as follows [15]

(5) $$C_{O2} = \dfrac{P_{O2}}{5.08\times10^6 e^{\frac{498}{T}}}$$

The Ohmic polarization loss is given as:

(6) $$V_{ohmic} = I R_m$$

R_m is ohmic resistance calculate in the paper [16, 18, 19]. A concentration polarization is expressed as:

(7) $$V_{con} = -B \times \ln(1 - \dfrac{I}{I_{lim}})$$

With I_{lim} being the current density where fuel is used in a same rate as the maximum input rate (A/cm^2).

To size the fuel cell, the amount of electric energy extracted from the FC should be calculated. Therefore, it is necessary to estimate the amount of energy generated from the FC per 1 Kg of hydrogen which can be obtained as follows [17]:

(8) $$E_g^{FC} = H_2^{used} \xi_{fc} \dfrac{H_2 heating value}{H_2 density}$$

Where H_2^{used} represents the quantity of hydrogen input to the FC in Kg, ζ_{fc} is the FC efficiency, H$_2$ heating value is equal to 3.4 kWh/m^3 in the standard condition and H$_2$ density is 0.09 Kg/m^3.

Modelling of solar PV

PV system is based on solar energy, where PV cell is the most basic generation part in PV. As figure 2 shows, the PV cell is formed from a diode and a current source was connected antiparallel with a series resistance [3].

The relation of the current and voltage in the single-diode cell can be written as follows:

(9) $$I_{PV} = I_{ph} - I_0\left(\exp\left(\dfrac{q(V_{PV} + R_{s\,mod} I_{PV})}{AKT}\right) - 1\right)$$
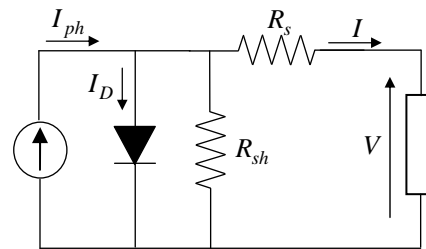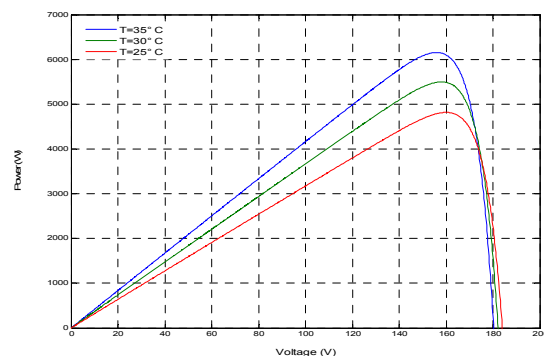

Fig. 2. Equivalent circuit of PV cell
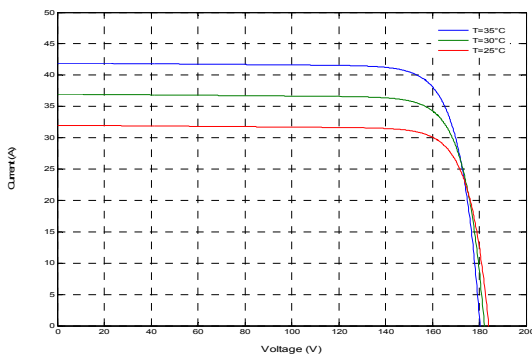

Fig. 3. Voltage-Power curve of PV panel

Fig. 4. Voltage-current curve of PV panel

DC/DC boost converter and Maximum Power Point Tracking (MPPT)

A boost converter is a step up DC/DC converter which increases the solar voltage to desired output voltage as required by load. The configuration is shown in figure 5, which consists of a DC input voltage V_{in}, inductor L, switch S, diode D1, capacitor C for filter, and load resistance R.

When the switch S is ON the boost inductor stores the energy fed from the input voltage source and during this time the load current is maintain by the charged capacitor so that the load current should be continuous. When the switch S is OFF the input voltage and the stored inductor voltage will appear across the load hence the load voltage is increased. Hence, the load voltage is depends upon weather switch S in ON or OFF and this is depends upon the duty ratio D.
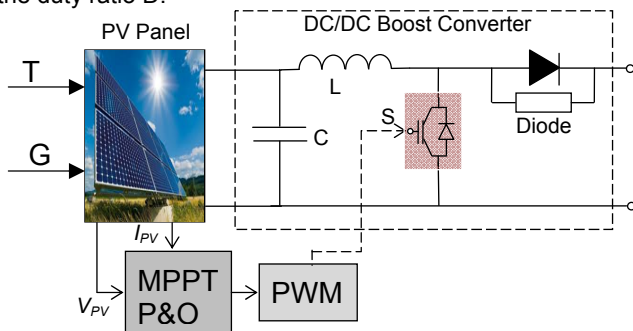

Fig. 5. Boost converter with MPPT control

The solar panel efficiency is increased by the use MPPT technique. The MPPT is the application of maximum power transfer theorem which says that the load will receive maximum power when the source impedance is equal to load impedance. The MPPT is a device that extracts maximum power from the solar cell and changes the duty ratio of DC/DC converter in order to match the load impedance to the source.

Battery Modelling

Several authors have proposed models for the battery and the results of experiments carried out on lead/acid batteries deduce a model named "CIEMAT model" representing the battery operation during the charge, discharge and overcharge processes. In our case study, from the carried out experiments, a validated model is proposed with respect to the battery capacity for any size and type of lead/acid battery [7, 11].

This model represented by an equivalent circuit model contains a voltage source which is the open circuit voltage

V, in series with an internal resistance R. Thus, the output voltage of the battery is:

$$(10) \qquad V_{bat} = V - RI_{bat}$$

where the both V_{bat} and I_{bat} depend on the battery state of charge (SOC), temperature and internal resistance variations R.
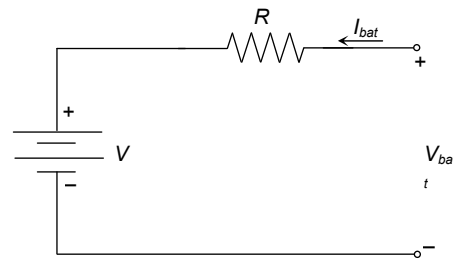

Fig. 6. The battery modelling

In this study, this simple model based on the CIEMAT model for the battery is considered as enough accurate to assess power management objectives and to compare performance of several strategies. During the charging and discharging process, the state of charge (SOC) in terms of time (t) can be described by [8]

$$(11) \qquad SOC(t) = \begin{cases} SOC(t - \Delta t) + P_{bat} \cdot \dfrac{\eta_{ch}}{C_n \cdot V_{dc}} \cdot \Delta t \\[2mm] SOC(t - \Delta t) + P_{bat} \cdot \dfrac{1}{\eta_{dis} \cdot C_n \cdot V_{dc}} \cdot \Delta t \end{cases}$$

where Δt is the time step, P_{bat} represents the battery power, C_n is the nominal capacity of the battery, η_{ch} and η_{dis} are respectively the battery efficiencies during charging and discharging phase. V_{dc} denotes the nominal DC bus voltage. At any time step Δt, the SOC must comply with the following constraints

$$(12) \qquad SOC_{min} \le SOC(t) \le SOC_{max}$$

where SOC$_{min}$ and SOC$_{max}$ are maximum and minimum allowable storage capacities, respectively.

Battery control

The objective of the control system is to regulate the battery current in order to obtain the required power.
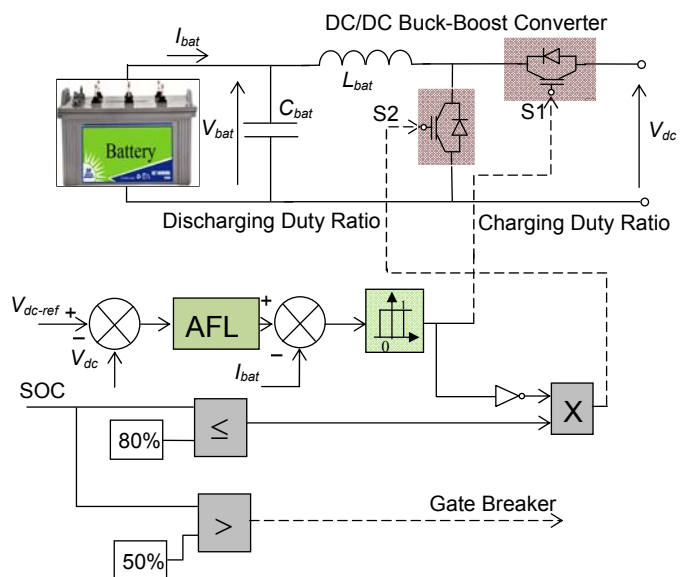

Fig. 7. The battery control using Adaptive Fuzzy Logic

Charging and discharging current limits and maximum SOC limitations are also included in the model. The BESS is connected to the DC grid via a bi-directional Buck-Boost DC/DC converter, as shown in figure 7.

Adaptive Fuzzy Logic Controller
The adaptive fuzzy-PI controller (AFLC-PI) is a conventional PI controller strengthened by a fuzzy logic algorithm. The proposed PI-based FLC is illustrated in Fig. 8. The desired output voltage and its derivative are the two input signals of the controller. The output signal is compared with a triangular waveform to generate a PWM signal for the buck converter duty cycle, which makes the actual voltage get as close as possible to the reference value in order to maximize the power. The scaling factors for the two input signals and for the output signal, K_e, K_{ce} and K_u respectively, are used to change the sensitivity of the fuzzy controller according to the fluctuating of battery voltage conditions without modifying the controller structure.
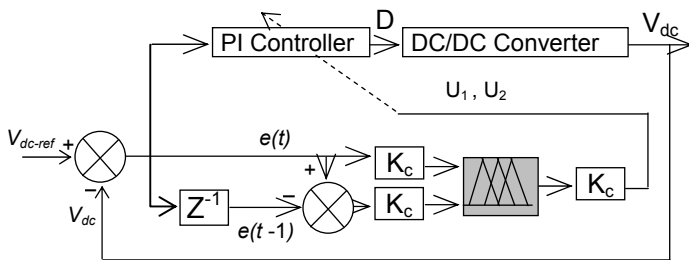

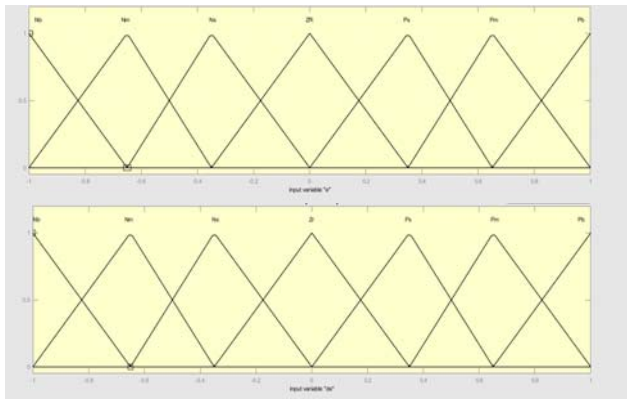Fig. 8. The battery modelling

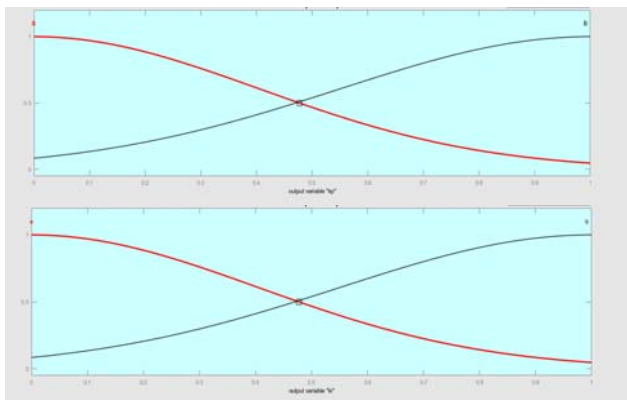Fig. 9. Error and change in error membership functions of FLC.

Fig. 10. Output membership functions of FLC.

The adaptive controller parameters are calculated using the following equations:

$$(13) \quad \begin{cases} K_{pF} = K_p U_1 \\ K_{iF} = K_i U_2 \end{cases}$$

where K_{pF} and K_{iF} are the fuzzy proportional and integral parameters; U_1 and U_2 are the adaptation gains.

In this study, a Mamdani-type fuzzy inference system is utilized in the fuzzy controller which is made up of three stages: fuzzification, inference system and defuzzification as presented in Figure 9 and 10 [9].

The 49 fuzzy control rules listed in Table 1 can be included into the fuzzy algorithm.

The fuzzy rules set displayed in Table 1 are chosen to increase or decrease the duty cycle depending on the error and its derivative, so as to achieve the reference value. The shaded rules in Table 1 can be read as follows:

‒ IF error (e) is (NB) and error change (ce) is (NB), the duty cycle should be increased (B).

‒ IF error (e) is (ZS) and error change (ce) is (NM), the duty cycle should be decreased (S).

Table 1. Set of fuzzy rules

U_1,U_2		ce						
		NB	NM	NS	ZR	PB	PM	PS
e	NB	B	B	B	B	B	B	B
	NM	S	B	B	B	B	B	S
	NS	S	S	B	B	B	S	S
	ZR	S	S	S	B	S	S	S
	PB	S	S	B	B	B	S	S
	PM	S	B	B	B	B	B	S
	PS	B	B	B	B	B	B	B

Power Management
The proposed chart of the power management system is described in figure 11, and it takes into consideration the following steps:

Step 1: define the different powers involved in our hybrid system,

Step 2: If the power supplied is greater than the requested power, in this case the excess power will be stored in the battery,

Step 3: If the requested power is greater than that generated, the following two cases are distinguish:

a) If the state of charge SOC is greater than 50 %, the storage battery devices are switched on.

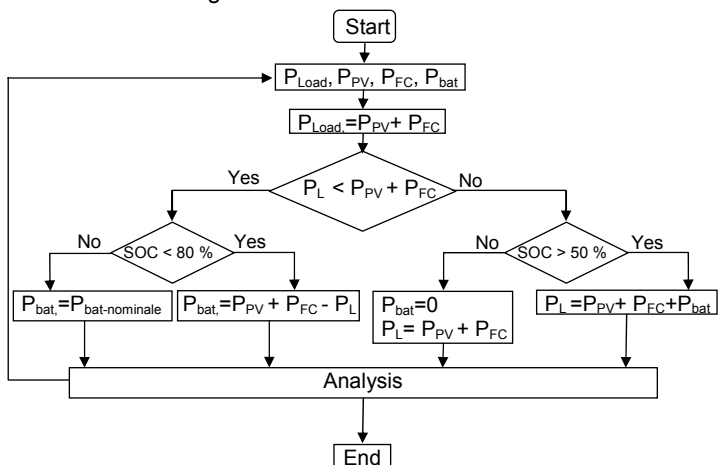b) In the opposite case, the battery stops working, which forces the delesting.

Fig. 11. Flow chart of the supervisory controller

Three level T Type Inverter Topology
Fig. 12 shows the schematic diagram of T Type-inverter topology. Each leg of a three-phase three-level T-type inverter is realised as an extension of conventional two-level VSI leg by using an active, bidirectional link between output and dc-link midpoint. Bidirectional link is can be a

series combination of two active switches connected in reverse direction as shown in Fig.12. Each inverter leg can be operated in one of the three switching states, where switching state represents a combination of operating status of each switch in a leg as shown in Table I. For a three-phase three-level T-type inverter, there are 33 = 27 possible switching state combinations [10, 21].

Table 2. Switching state

Switching state S	Switch status (x=a, b, c)				Pole voltage Vxz
	Tx1	Tx2	Tx3	Tx4	
P	ON	ON	OFF	OFF	+0.5 Vdc
O	OFF	ON	ON	OFF	0
N	OFF	OFF	ON	ON	-0.5 Vdc

Each switching state combination is defined as Vi = [Ta Tb Tc], where Sx(x = a,b,c) is the switching state of the corresponding leg and Vi is the voltage vector formed by the ith switching state combination.
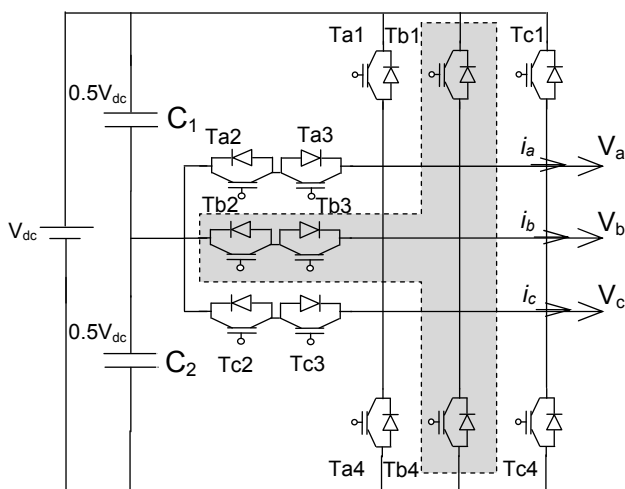

Fig. 12. Three level T Type inverter topology

Simulation Results

The simulations carried out to check the validity of the proposed scheme used Adaptive Fuzzy Logic Control (AFLC) to control the DC voltage of the batteri connected to the multi-sources (PV-FC) system integrated with an AC load.

It is evaluated using MATLAB/Simulink software under variable load conditions. The proposed system parameters are listed in Table 3, 4, 5 and 6.

The proposed system is operated in three possible operating modes depending on the variable load.

Simulation tests were performed in the following cases as shown in the figure 13:

Case 1: from 0 s at 3 s (corresponds to a morning period)

We have imposed a demanded average load of 10 kW, we have a reduced sunshine of 600 W/m^2. The photovoltaic generator produces an energy of 5 kW. To compensate for the rest of the energy required the fuel cell and the battery will react such as the first decreasingly and the second increasing.

Case 2: from 3 s at 7.5 s (afternoon period)

In this period, we see that we have a reduced consumption of 7 kW. The following scenarios are noted:
Between 3 s and 4.5 s: low irradiation of 600 W/m^2 and the fuel cell is disconnected so the PV and the battery provide the requested energy.

Between 4.5 s and 6 s: an irradiation increase linearly from 600 W/m^2 to 1000 W/m^2, the fuel cell remains disconnected, the PV and the battery react in opposite ways to ensure the power of 7 kW.

Between 6 s and 7.5 s: the battery being always disconnected, the irradiation decreases linearly, the PV and the battery always have an opposite reaction all while covering the requested energy.

Case 3: (The evening)

This period represents a strong demand for power and contain two phases:

Phase 1: P$_{Load}$=14 kW, disconnected fuel cell, E=600 W/m^2, which implies that the PV generates 5 kW and the rest of requested power (9 kW) is delivered by the battery.

Phase 2: the load continues to increase until waiting for a value of 16 kW, all sources are active, the PV always gives 5 kW, the fuel cell and the beetery cover the strong charging power required
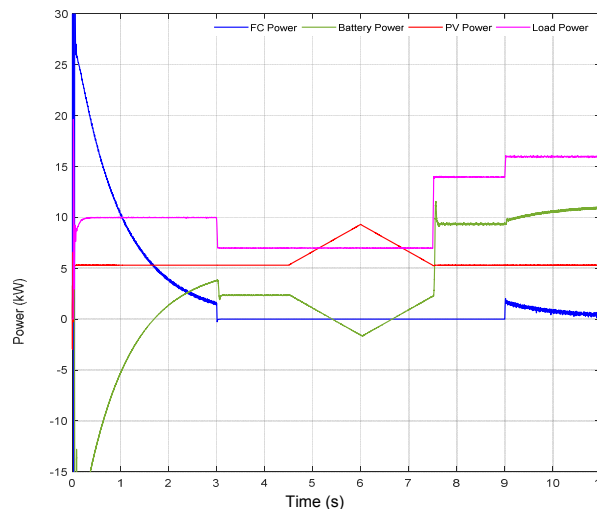

Fig. 13. Power generation of the hybrid system under varying AC load

In figure 14, we present the global (total) state of charge SOCG of storage devices. From 0 s to 7.5 s the SOC equals 60%, and the system operates with full charge. All the storage devices are switched off because the total fuel cell and PV generated power is higher than the load demand as shown in figure 13.

When a SOCG decreases, and the system enters the critical mode. The supervisory controller reacts properly and switches off the load of the lowest priority in order to save the equilibrium of the overall system. If we have lack of power, we have to request for the utility of delesting process, and hence, all storage devices would be disconnected. Else, we authorize the charge mode of the storage system.

The Figures 16 respectively show the current and the voltage of the load, they are purely sinusoidal.

As it can be seen in Figure 17, with changing power, the DC link voltage V_{dc} is well kept constant at the specified value (640V) which constitutes an important advantage and proves the effectiveness of the proposed schema. It has allowed us to equalize the different input DC link voltages of the multilevel inverter. Then, the input voltages are practically equal by pairs as shown in figure 17.
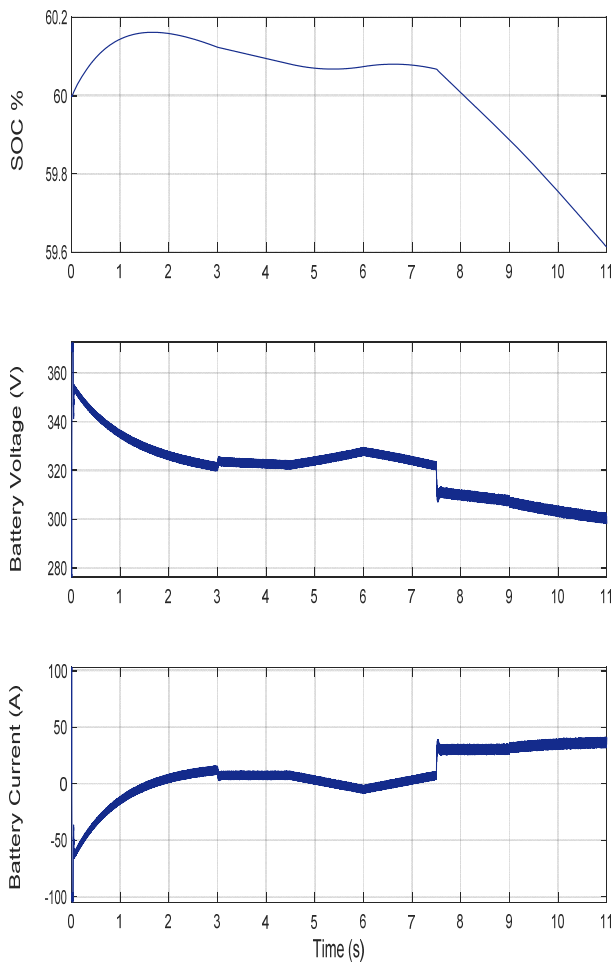
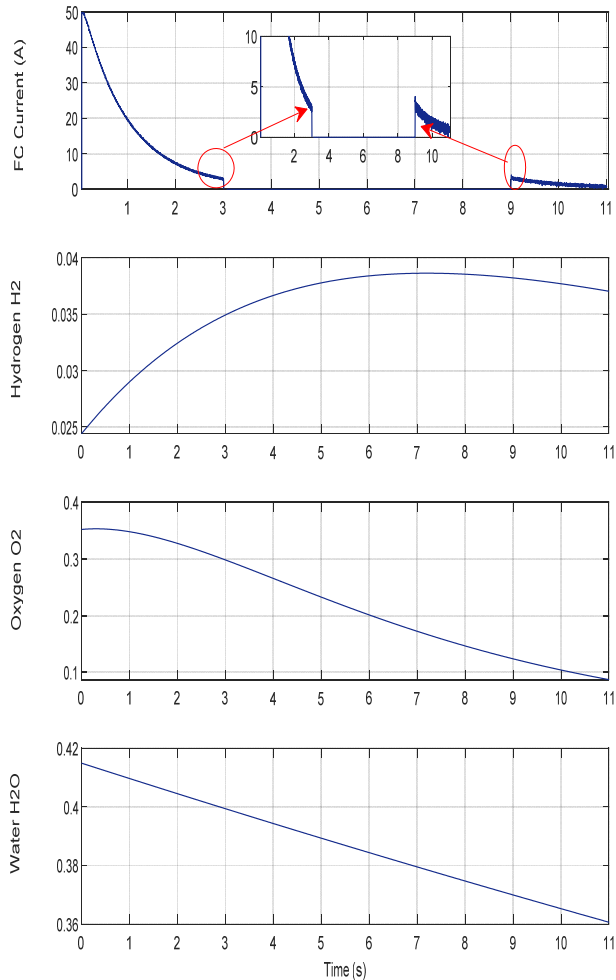Fig. 14. Global state of charge of battery, voltage and current battery

Fig. 15. Output voltage and current for inverter

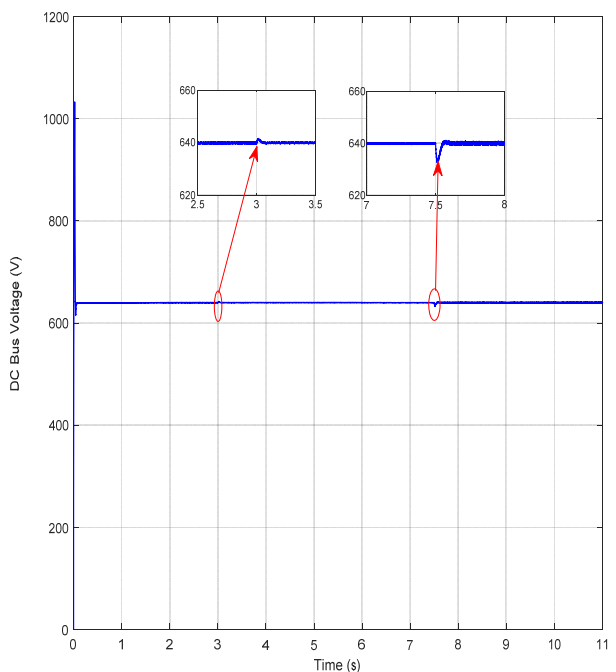Fig. 16. Fuel cell current, hydrogen and water characteristics
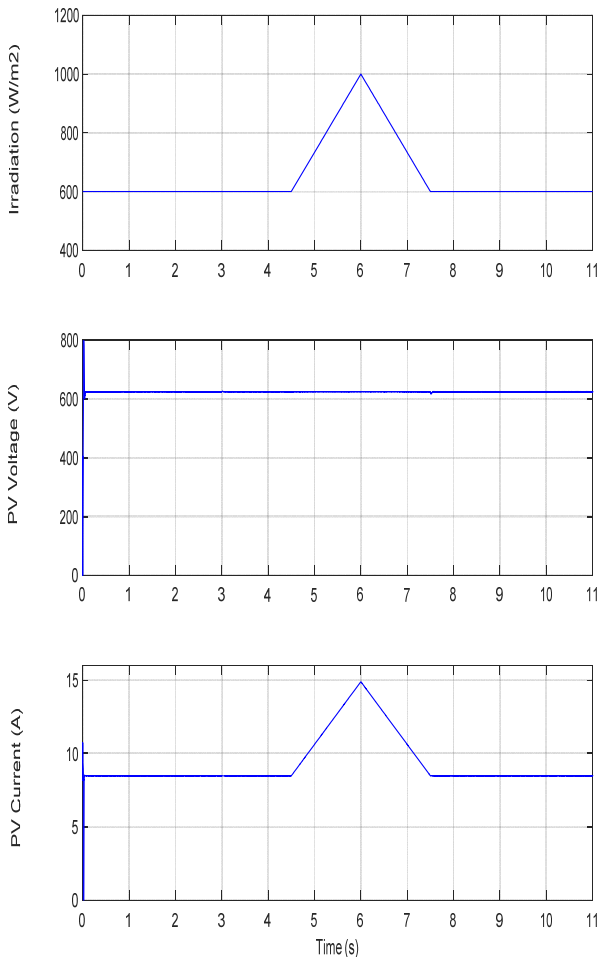

Fig. 17. DC bus voltage

Fig. 18. Irradiation, PV voltage and current

Figures 16 and 18 shows the characteristics of the fuel cell and PV system under the variation of the AC load.

These results show the efficiency of the management and the controls used for this hybrid system compared with another classical method.

Conclusion

In this paper a multi source energy system for hybrid PV/FC energy and battery have been presented. Dynamic modeling and simulations of the hybrid system is proposed using SIMULINK. A hybrid energy system and its supervisory-control system was developed and tested. Load demand is met from the combination of PV array, Fuel Cell and the battery. A three level T type inverter is used to convert output from solar and fuel cell systems into AC power output. Circuit Breaker is used to connect and disconnet an additional load in the given time. This hybrid system is controlled to give maximum output power under all operating conditions to meet the load. Either solar or fuel cell system is supported by the battery to meet the load. Also, simultaneous operation of fuel cell and solar system is supported by battery for the same load.
These results show the efficiency of the management and the controls used for this hybrid system and can be implemented easily with DSP or Dspace platform.

Appendix

Table 3. Battery and AC Load Parameters

Components	Rating values
Load 1, 2, 3 (R)	7 kW, 7 kW, 3 kW
Battery type	Nickel Metal hydride
Nominal voltage	300 V
Capacity rating	6.5 AH

Table 4. Fuell Cell Paramaters

Absolute temperature (K)	1273
Initial current (A)	50
Faraday's constant (C/kmol)	96.487e6
Universal gas constant J/(kmol K)	8314
Ideal standard potential (V)	1.18
Number of cells in series	450
Maximum, minimal and optimal fuel utilization	[8.43e-4 2.81e-4 2.52e-3]
Response time for hydrogen, water and oxygen flow (s)	[26.1 78.3 2.91]
Ohmic loss per cell (ohms)	3.2813e-004
Electrical response time (s)	2
Fuel processor response time (s)	5
Ratio of hydrogen to oxygen	0.145

Table 4. PV Parameters

Components	Rating values
Peak Power	200 W
Peak Voltage	660 V
Peak current	7.52 A
Open Circuit Voltage	33.2 V
Short Circuit Current	8.36 A

Table 6. Three level T Type Inverter

Components	Rating values
$C_1 = C_2$	2.2 mF
Dc link Voltage	640 V
Frequency	50 Hz
Converter Inductor	5 mH
DC link Voltage	640 V
Converter Capacitor	2.2 mF

Authors *Mostefa Koulali, University Tahar Moulay of Saida, Adresse:BP 138 cité ENNASR 20000, Saida, Algeria, mostefa.koulali@univ-tiaret.dz*
Karim Negadi, Laboratory of Energy and Computer Engineering L2GEGI, Department of Electrical Engineering, Faculty of Sciences Applied, University Ibn Khaldoun of Tiaret, BP 78 Size Zarroura, Tiaret 14000, Algeria, karim.negadi@univ-tiaret.dz
Mohamed Mankour, Electrotechnical Engineering Laboratory, University Tahar Moulay of Saida, Adresse: BP 138 cité ENNASR 20000, Saida, Algeria, mankourmohamed312@yahoo.fr
Abdelkader Mezouar, Electrotechnical Engineering Laboratory, University Tahar Moulay of Saida, Adresse:BP 138 cité ENNASR 20000, Saida, Algeria, Algeria, a.mezouar@yahoo.fr
Abderrahmane Berkani, Laboratory of Energy and Computer Engineering L2GEGI, Department of Electrical Engineering, Faculty of Sciences Applied, University Ibn Khaldoun of Tiaret, BP 78 Size Zarroura, Tiaret 14000, Algeria, abderrahmane.berkani@univ-tiaret.dz
Bachir Boumediene, Laboratory of Energy and Computer Engineering L2GEGI, Department of Electrical Engineering, Faculty of Sciences Applied, University Ibn Khaldoun of Tiaret, BP 78 Size Zarroura, Tiaret 14000, Algeria, bachir.boumediene@univ-tiaret.dz

REFERENCES
[1] G. Eason, B. Noble, and I. N. Sneddon, "On certain integrals of Lipschitz-Hankel type involving products of Bessel functions," Phil. Trans. Roy. Soc. London, vol. A247, pp. 529–551, April 1955. (references)
[2] J. Clerk Maxwell, A Treatise on Electricity and Magnetism, 3rd ed., vol. 2. Oxford: Clarendon, 1892, pp.68–73.
[3] I. S. Jacobs and C. P. Bean, "Fine particles, thin films and exchange anisotropy," in Magnetism, vol. III, G. T. Rado and H. Suhl, Eds. New York: Academic, 1963, pp. 271–350.
[4] Nabil Karami , NazihMoubayed , RachidOutbib ,Energy management for a PEMFC–PV hybrid system, http://dx.doi.org/10.1016/j.enconman.2014.02.070, Energy Conversion and Management 82 (2014) 154–168.
[5] V. Boscaino, R. Miceli, G. Capponi, G. RiccoGalluzzo, A review of fuel cell based hybrid power supply architectures and algorithms for household appliances, 0360-3199/$ e see front matter Copyright ª 2013, Hydrogen Energy Publications, LLC. Published by Elsevier Ltd, http://dx.doi.org/10.1016/j.ijhydene.2013.10.165.

[6] Th.F. El-Shatter, M.N. Eskandar, M.T. El-Hagry, Hybrid PV/fuel cell system design and simulation, 0960-1481/02/$ - see front matter 2002 Elsevier Science Ltd, PII: S09 60 -1481(01)00062-3, Renewable Energy 27 (2002) 479–485.

[7] PhatiphatThounthong, ArkhomLuksanasakul, PoolsakKoseeyaporn, Intelligent Model-Based Control of a Standalone Photovoltaic / Fuel Cell Power Plant With Supercapacitor Energy Storage, IEEE Transactions on Sustainable Energy, VOL. 4, NO. 1, January 2013, 1949-3029/$31.00 © 2012 IEEE.

[8] Akbar Maleki, AlirezaAskarzadeh, Optimum Configuration of Fuel Cell-B PV/Wind Hybrid System using a Hybrid Metaheuristic Technique, International Journal of Engineering & Applied Sciences (IJEAS) Vol.5, Issue 4 (2014)1-12.

[9] Aicha Asri, Youcef Mihoub, Said Hassaine, Pierre-Olivier Logerais, Adel Amiar, Tayeb Allaoui, an adaptive fuzzy proportional integral method for maximum power point tracking control of permanent magnet synchronous generator wind energy conversion system, Rev. Roum. Sci. Techn.– Électrotechn. et Énerg. Vol. 63, 3, pp. 320–325, Bucarest, 2018

[10] Ronak V Nemade, Reconfiguration of T-type Inverter for Direct Torque Controlled Induction Motor Drives under Open Switch Faults, 0093-9994 (c) 2016 IEEE, DOI 10.1109/TIA.2016.2628721, IEEE.

[11] Abderrahmane Berkani, Karim Negadi, Tayeb Allaoui, Fabrizio Marignetti, , Sliding Mode Control of Wind Energy Conversion System Using Dual Star Synchronous Machine and Three Level Converter, TECNICA ITALIANA-Italian Journal of Engineering Science, Vol. 63, No. 2-4, June, 2019, pp. 243-250.

[12] M. Caldero´n, A.J. Caldero´n, A. Ramiro, J.F. Gonza´lez, Automatic management of energy flows of a stand-alone renewable energy supply with hydrogen support, International Journal of hydrogen energy 3 5 (2 0 1 0) 2 2 2 6 – 2 2 3 5.

[13] ErkanDursun, Osman Kilic, Comparative evaluation of different power management strategies of a stand-alone PV/Wind/PEMFC hybrid power system, 0142-0615/$ - see front matter _ 2011 Elsevier Ltd. doi:10.1016/j.ijepes.2011.08.025, Electrical Power and Energy Systems 34 (2012) 81–89.

[14] Juan P. Torreglosa, PabloGarcía-Triviño, Luis M. Fernández Ramirez, Francisco Jurado, Control based on techno-economic optimization of renewable hybrid energy system for stand-alone applications, http://dx.doi.org/10.1016/j.eswa.2015.12.038 0957-4174/© 2016 Elsevier Ltd, Expert SystemsWith Applications 51 (2016) 59–75.

[15] Jingang Han, Jean-Frederic Charpentier and Tianhao Tang, An Energy Management System of a Fuel Cell/Battery Hybrid Boat, Energies 2014, 7, 2799-2820; doi:10.3390/en7052799.

[16] Omar Hazem Mohammed, YassineAmirat, Mohamed Benbouzid, Adel Elbast. Optimal Design of a PV/Fuel Cell Hybrid Power System for the City of Brest in France.IEEE ICGE 2014, Mar 2014, Sfax, Tunisia.pp.119-123. hal-01023490.

[17] Pablo García, Juan P. Torreglosa, Luis M. Fernández , Francisco Jurado, Improving long-term operation of power sources in off-grid hybrid systems based on renewable energy, hydrogen and battery, Journal of Power Sources 265 (2014) 149e159.

[18] A. Elbaset, Design, Modeling and Control Strategy of PV/FC Hybrid Power System, Journal of Electrical System 7.2 (2011): 270-286.

[19] Pablo Garc´ı´a, Juan P. Torreglosa, Luis M. Ferna´ndez, Francisco Jurado, Optimal energy management system for standalone wind turbine/photovoltaic/hydrogen/battery hybrid system with supervisory control based on fuzzy logic, http://dx.doi.org/10.1016/j.ijhydene.2013.08.106, International Journal of Hydrogen Energy 38 (2013) 14146-14158.

[20] Power management system for off-grid hydrogen production based on uncertainty, International Journal of Hydrogen Energy 40 (2015) 7260 -7272.

[21] Mostefa Koulali, Mohamed Mankour, Karim Negadi, Abdelkader Mezouar, Energy Management of Hybrid Power System PV Wind and Battery Based Three Level Converter, TECNICA ITALIANA-Italian Journal of Engineering Science Vol. 63, No. 2-4, June, 2019, pp. 297-304.